DISTRIBUTION OF METHANE IN THE GULF OF MEXICO

An Undergraduate Research Scholars Thesis

by

HAYLEY BREY

Submitted to the Undergraduate Research Scholars program
Texas A&M University
in partial fulfillment of the requirements for the designation as an

UNDERGRADUATE RESEARCH SCHOLAR

Approved by
Research Advisor: Dr. Shari Yvon-Lewis

May 2016

Major: Environmental Geoscience

TABLE OF CONTENTS

ABSTRACT

Distribution of Methane in the Gulf of Mexico

Hayley Brey
Department of Geosciences
Texas A&M University

Research Advisor: Dr. Shari Yvon-Lewis
Department of Oceanography

Methane (CH_4) originating from thermogenic (e.g. seafloor seeps) and biogenic sources (e.g. methanogenesis) affects the distribution of methane concentrations at varying depths in the ocean. A comprehensive survey of CH_4 concentrations throughout the Gulf of Mexico has been difficult to obtain due to international boundaries. For this study, samples were collected from the Northern and Western Gulf of Mexico, including areas within the Mexican Exclusive Economic Zone (EEZ). These samples were analyzed for CH_4, ethane (C_2H_6), and propane (C_3H_8). The vertical and areal distribution of CH_4 in the Gulf of Mexico is assessed. The lack of measurable concentrations of C_2H_6 and C_3H_8 in the samples suggest that there were no thermogenic sources. Methane concentrations were elevated in profiles with lower dissolved oxygen concentrations at the oxygen minimum. The calculated sea-to-air flux of CH_4 averaged 19.1 μmol m^{-2} d^{-1} in the Northern Gulf of Mexico and is in agreement with previous measurements. For the Western Gulf of Mexico, where there is no prior reported surface CH_4 data, the sea-to-air flux averaged 115.2 μmol m^{-2} d^{-1}.

ACKNOWLEDGMENTS

I would like to thank Charlotte Woods, Jordan Young, and Constance Preveti for their assistance in collecting and processing samples. I reserve special thanks for Dr. Shari Yvon-Lewis for mentoring me and being an amazing thesis advisor.

NOMENCLATURE

GC	Gas Chromatograph
FID	Flame Ionization Detector
GOM	Gulf of Mexico
EEZ	Exclusive Economic Zone
GISR	Gulf Integrated Spill Research
CH_4	Methane
CO_2	Carbon Dioxide
C_2H_6	Ethane
C_3H_8	Propane
O_2	Oxygen
DOM	Dissolved Organic Matter
$HgCl_2$	Mercuric Chloride
G05	Cruise mainly in the EEZ of Mexico
G06	Cruise in the Northern Gulf of Mexico

CHAPTER I

INTRODUCTION

Methane (CH_4) is the most abundant hydrocarbon in the atmosphere [*Reeburgh*, 2007]. The global warming potential of CH_4 is twenty-three times that of carbon dioxide (CO_2) [*Brown et. al.*, 2014]. Since pre-industrial times, methane has contributed approximately 20% to the Earth's warming [*Karl et. al.*, 2008]. Methane makes up 0.0002% of the atmosphere, while CO_2 makes up 0.035% [http://www.met.fsu.edu/orgs/explores/atmcomp.html]. Carbon dioxide has a larger impact than CH_4 even though it has a smaller global warming potential than methane, because there is much more CO_2 emitted into the atmosphere.

Observations of oceanic dissolved CH_4 concentrations have only been available for the last 60 years [*Reeburgh*, 2007]. The atmosphere and ocean are not in equilibrium with respect to gas concentrations, including CH_4. If the ocean is undersaturated, it is a sink for atmospheric methane, taking methane out of the atmosphere. If the ocean is supersaturated, it becomes a source of methane to the atmosphere. Globally, The ocean acts as a source of CH_4 and as the oceans are a source and are thought to contribute to 1-4% of annual global CH_4 emissions [*Karl et. al.*, 2008].

The exchange or flux of gases across the air-sea interface is controlled by the concentration gradient between the surface ocean and atmosphere and the wind speed. Gases are exchanged between the atmosphere and ocean even if they are in equilibrium. The unstirred laminar boundary layer is a significant barrier to this exchange on a molecular level. The thickness of this

layer varies with wind speed and sea state (up to 100μm). The gradient across this layer controls the mixing between the well-mixed atmosphere above and the well-mixed ocean below [*Libes,* 2009].

Methane sources to the ocean are classified as biogenic or thermogenic. Biogenic CH_4 comes from biological processes such as methanogenesis. Thermogenic sources include emissions from natural seeps on the seafloor as well as losses from oil and gas production. If there are detectable dissolved concentrations of both ethane (C_2H_6) and propane (C_3H_8) with the CH_4 the source of CH_4 is likely thermogenic [*Etiope et al.*, 2014]. If there are no detectable levels of C_2H_6 and C_3H_8, the CH_4 is likely biogenic [*Karl et. al.*, 2008].

Methanogenesis is one of the pathways for dissolved organic matter (DOM) oxidation in the ocean. Aerobic respiration yields the highest amount of energy of all oxidation reactions and is most favored in areas with available oxygen (O_2). As oxygen becomes less available other reactions become more preferred. When O_2, manganese dioxide (MnO_2), nitrate (NO^{3-}), iron (Fe^{3+}), and sulfate (SO_4^{2-}) become depleted or less available methanogenesis becomes a possible reaction pathway (Libes, 2009). Methanogenesis, or methane fermentation, produces the smallest amount of energy of all the heterotrophic DOM oxidation processes in the ocean and follows the reaction (equation 1) [adapted from *Sarimento and Gruber* (2006)];

$$DOM + 59\ H_2O \rightarrow 47\ CO_2 + 59\ CH_4 + 16\ NH_3 + H_3PO_4 \qquad (1)$$

Where DOM= $C_{106}H_{175}O_{42}N_{16}P$ [*Anderson,* 1995]

This reaction results in some of the carbon in organic matter being oxidizing to CO_2 and some being reduced to CH_4. This is a bacterially mediated process.

Natural seafloor seeps are sources of thermogenic oil and gas, including CH_4, C_3H_8, and C_2H_6. The oil and gas originates from sub-seafloor reservoirs and escapes the seafloor in the Gulf of Mexico because of salt tectonics [*MacDonald et al.*, 2003]. These gases can also be introduced into the water column from industrial discharge and oil spills. Methane emissions from the seafloor are a natural source of methane that may affect methane fluxes to the atmosphere. The Gulf of Mexico is a region with a large number of natural seeps. When natural seeps release methane in the form of gas bubbles the methane is oxidized as the bubble rises [*Tsunogai et. al.* 2010].

CHAPTER II

METHODS

Sampling Stations

Samples were collected during from two cruises conducted aboard the R/V Pelican in the Gulf of Mexico during August 2013 (G05) and June 2014 (G06) (Figure 1 & 2). These cruises were part of a series of cruises conducted for the Gulf Integrated Spill Research (GISR) Consortium project. A set of twelve niskin bottles were deployed to take samples from various depths at the stations sampled. The depths sampled ranged from the surface to over 2,000 meters deep. The methane samples were collected and stored in a 100 mL crimp topped serum bottle with no headspace. The samples were not analyzed on board; they were poisoned with saturated mercuric chloride ($HgCl_2$) and stored in a cold room. Temperature, salinity, and dissolved oxygen concentrations were also measured for these profiles.

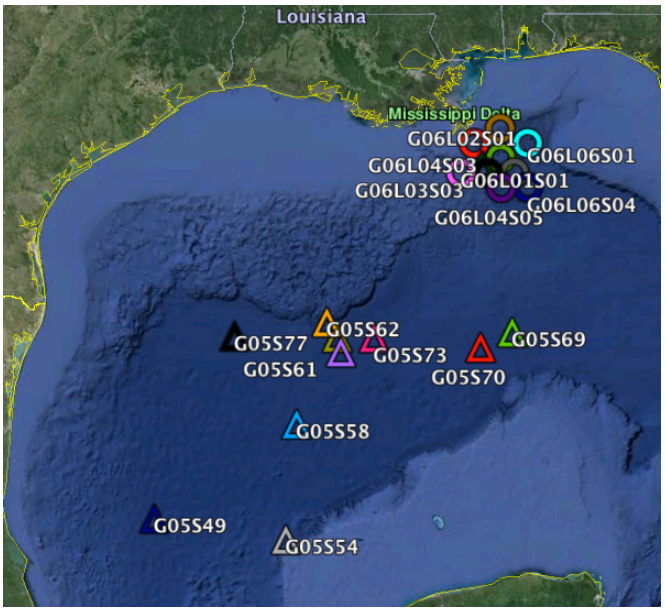

Figure 1: Map of Northwestern Gulf of Mexico. The G05 stations are shown as triangles, and the G06 stations are

Figure 2: Close up view of stations located in the Northern Gulf of Mexico.

Methane Analysis

For each sample, a headspace of approximately 20 mL is introduced; the exact number was recorded up to a tenth of a milliliter. This was done by connecting a 10 mL glass syringe and a tedlar, or mylar, gas-sampling bag full of nitrogen gas. A very small amount of water, approximately .2 mL, was removed using the gas syringe. Then the valve on the tedlar bag was opened. A small amount was first removed to prevent water from potentially entering into the tedlar bag and contaminating it. Once the tedlar bag valve is open and nitrogen is free to move into the sample, the syringe is used to pull out the closest amount to 10 mL of water as possible. This is done twice. The valve on the tedlar bag is then closed and the needle is removed. The needle on the tedlar bag and the glass syringe are wiped down with a chem-wipe and have clean nitrogen blown through them to clean them between bottles. This is done for every sample analyzed. The bottles are then left for 1-3 days so that the headspace and the water could equilibrate according to the Ideal Gas Law. Gas from the equilibrated headspace is extracted and

injected into the gas chromatograph with flame ionization detector (GC/FID). The room temperature is recorded on the day the headspace was analyzed, for determining solubility.

The GC/FID has to be continuously run to ensure accurate results. A couple of room air injections are done to get the instrument started. Then, a calibration curve is run. Two rounds of zero air were run through the GC/FID. Then two rounds of calibration one, then two rounds of calibration two and two rounds of calibration three were ran. These standards are stored in gas tanks and hooked up to the GC/FID when needed. These standards have to be run before any samples can be. These values (Table 1) are later used to determine the calibration curve.

Table 1: Standard Calibrations Value

Calibrations:	**CH_4 (ppm)**	**CH_4 (atm)**
Zero Air	0	0
Calibration 1	0.99	0.00000099
Calibration 2	2.96	0.00000296
Calibration 3	6.1	0.0000061

An aliquot of the equilibrated headspace is injected into the GC/FID. A tedlar bag full of nitrogen gas was connected to the sample by a needle to replace the removed headspace and maintain ambient pressure. The tedlar bag valve was opened and headspace was removed using a plastic 10 mL plastic syringe, approximately 8-10 mL was removed. The syringe was removed and the tedlar bag valve was closed. The needle was removed from the syringe and the syringe was placed in the GC/FID injection port. Once the GC/FID was ready the sample was pushed from the syringe into the GC/FID loop at a consistent pace. The GC/FID was then run. The

needle on the syringe and bag was flushed with nitrogen and wiped down with a chem-wipe between each sample. The barometric pressure was read and recorded in millibar (mb) at the time each sample was run and was later converted to atmospheres (atm). The GC/FID's loop temperature was recorded for each sample originally in Celsius and later converted to Kelvin.

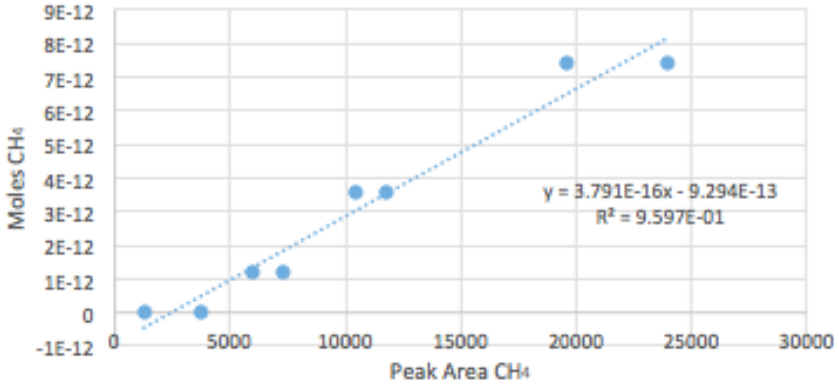

Figure 3: Representative Calibration Curve

The Ideal Gas Law is used to find the total mass (moles) sample gas present in the loop for each injection and is shown below in equation 2:

$$pV = nRT \qquad (2)$$

Where R is the gas constant and equals .082 $L \cdot atm \cdot mol^{-1} \cdot K^{-1}$, V is a constant equal to .00003 L (for methane), p is the barometric pressure of the room at the time the sample was run in atmospheres, T is the GC/FID loop temperature in Kelvin, and n is the total moles in the loop is represented by n. The equation produced from the calibration curve (Figure 3), for the day the sample was run, and utilized to find the total number of moles of methane in the loop for the

sample. This was done by using the area under the curve from the GC/FID representing methane as the x in the linear regression fit to the calibration data. The head space partial pressure (atm), or mixing ratio (mol mol^{-1}), was determined by dividing the total moles of CH_4, as determined from the calibration curve, by the total moles of headspace gas in the loop for a sample.

The CH_4 solubility (K_H) was calculated for each sample as shown below in equation 3:

$$\ln(\beta) = A_1+A_2(100/T)+A_3\ln(T/100)+A_4(T/100)^2+S\cdot[B_1+B_2(T/100)+B_3(T/100)^2] \quad (3)$$

Where β is the Bunsen coefficient (mL/L), T is the sample analysis temperature (K), S is salinity (‰), and A_1, A_2, A_3, A_4, B_1, B_2, B_3 are constants [*Wiesenburg and Guinasso,* 1979)] (Table 2). Bunsen is converted to K_H by:

$$K_H = (\beta)/(RT/P) \quad (4)$$

Where β is the Bunsen coefficient (Equation 3), R is the Gas Law constant, T is the sample analysis temperature (K), P is the atmospheric pressure (atm), K_H is the Henry's Law Constant ($mol\cdot L^{-1}\cdot atm^{-1}$) for the sample. The water concentration ($mol\cdot L^{-1}$) of CH_4 is found by multiplying the Henry's Law constant by the partial pressure of CH_4 in the equilibrated headspace for each sample. The total number of moles in the water is found by multiplying the water concentration by the volume of water (L) after the headspace was taken.

Table 2: Constant Values for Henry's Law

Variable	Value
A_1	-68.8862
A_2	101.4956
A_3	28.7314
A_4	-
B_1	-0.076146
B_2	0.043970
B_3	-0.068672

Source: *Wiesenburg and Guinasso* [1979]

The total moles of gas in the headspace was determined using the Ideal Gas Law (Equation 2). This time p is the barometric pressure of the room at the time the sample was run in atmospheres, V is the volume of the headspace (approximately .02 L), R is the gas constant (0.082 $L \cdot atm \cdot mol^{-1} \cdot K^{-1}$), T is the sample analysis temperature in Kelvin, n is the total moles of gas in the headspace. The total moles of methane in the headspace was found by multiplying the total moles of gas in the head space by the partial pressure of the head space. The total mass of methane in the original sample is distributed between the equilibrated headspace and the water. The masses of CH_4 in the equilibrated headspace and dissolved in the water are added together and then divided by the volume of water (L) to find the total concentration of methane in the original sample before equilibration with the added nitrogen headspace.

Flux calculations

The net sea-to-air flux (F) of a gas across the air-sea interface is determined from the following equation (equation 5):

$$F = K_W \left(C_W - \frac{p_a}{H} \right) \quad (5)$$

Where K_w is the gas exchange coefficient (m d^{-1}), C_w is the surface water concentration (mol m^{-3}) of the gas, p_a is the partial pressure (atm) of the gas in the overlying atmosphere, and H is the solubility (mol m^{-3} atm^{-1}) of the gas. The p_a is the monthly global average methane atmospheric pressure at the time of the cruise [ftp://aftp.cmdl.noaa.gov/products/trends/ch4/ch4_mm_gl.txt] (Table 3). The value for August 2013 (G05) was 1807.7 ppb and ppb 1818.5 for June 2014 (G06)

Table 3: NOAA's Monthly Global Average Methane

Date:	Global Average CH_4 (ppb)
August 2013	1807.8
June 2014	1818.5

Calculating the gas exchange coefficient

The gas exchange coefficient (K_w) is calculated using the equation 6 below:

$$K_w = K_{660}\left(\frac{Sc}{660}\right)^{-0.5} \quad (6)$$

Where K_{660} is determined using equation 7 and the Schmidt number conversion (Sc) is calculated using equation 8, both shown below:

$$K_{660} = 0.27U^2 \qquad \text{[Sweeney et al., 2007]} \qquad (7)$$

$$Sc = 2301.1 - 151.1T + 4.7364T^2 - 0.059431T^3 \quad (8)$$

Where U is the 10 meter wind speed (m s^{-1}) obtained from averaging values from surrounding moorings over the sampling dates from each cruise. The average wind speed for G05 was 5 m s^{-1} and the G06 value was 5.5 m s^{-1}. The 0.27 is the Sweeney gas exchange coefficient in cm hr^{-1}. The T is the temperature (C) of the surface water sampled at the time of sampling.

CHAPTER III

RESULTS & DISCUSSION

Methane Concentrations

Profiles displaying CH_4 concentrations from G05 and G06 are shown below in Figures 4 and 5. The maximum for G05 is 248.6 nmol/L and occurs at station G05S70. The maximum for G05 is 25.2 nmol/L and occurs at station G06L04S01. There were no measurable concentrations of C_2H_6 or C_3H_8 in samples from either cruise. The lack of measurable ethane and propane concentrations suggest that there were no thermogenic sources. This is in contrast to previous studies preformed in the Gulf of Mexico with measurable C_2H_6 and C_3H_8 levels [*Frank et al.*, 1970]. Station G05S87 is from G05 but is located in the Northern Gulf of Mexico near the G06 stations (Figure 2). The northern Gulf of Mexico and western Gulf of Mexico is defined by Table 4. The northern Gulf of Mexico is a region abundant with natural seeps [*MacDonald et al.,* 2015]. The results displayed relatively higher methane concentrations in parts of the western Gulf of Mexico than the northern Gulf of Mexico (Figure 4 & 5).

Table 4: Stations defined by regions.

Region:	Stations
Northern Gulf of Mexico	G06L01S01, G06L03S03, G06L04S05, G06L06S04, G06L05S04, G06L06S01, G06L04S03, G06L02S01, G06L04S01, and G05S87
Western Gulf of Mexico	G05S49, G05S54, G05S58, G0561, G05S62, G05S69, G05S70, G05S73, G05S74, and G05S77

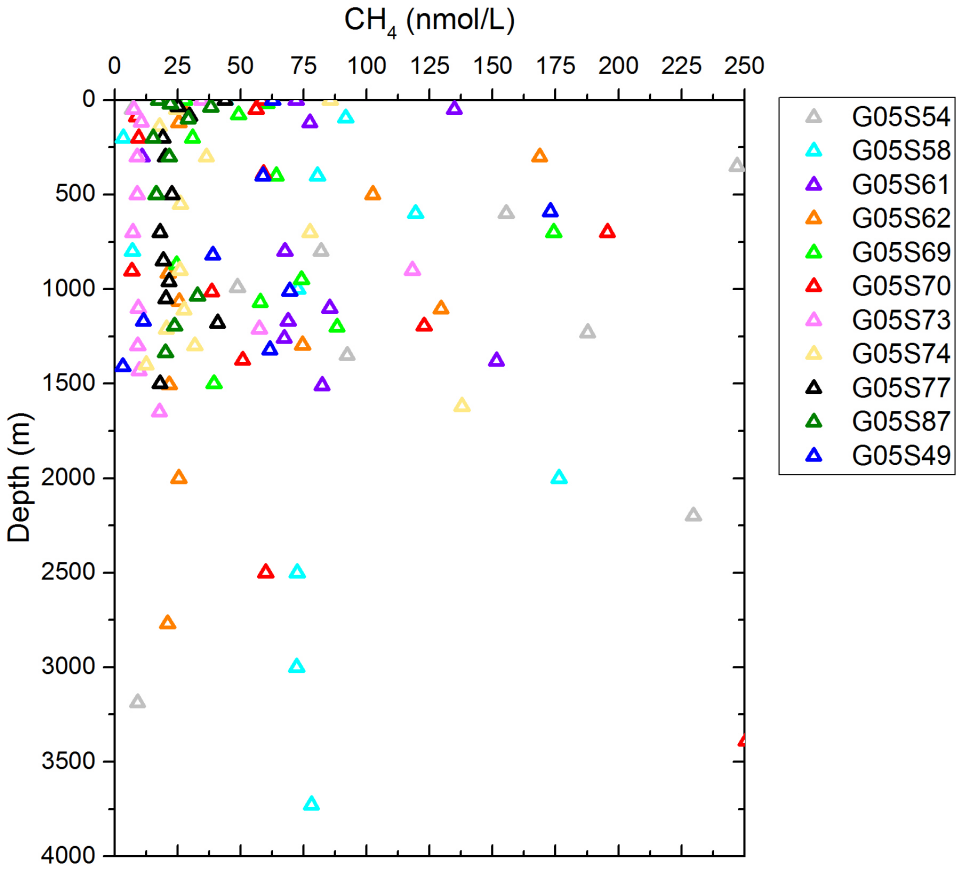

Figure 4: Methane concentrations from G05, represented by the triangular symbols. The colors of the station symbols match those used in Figure 1 & 2 that showed station locations.

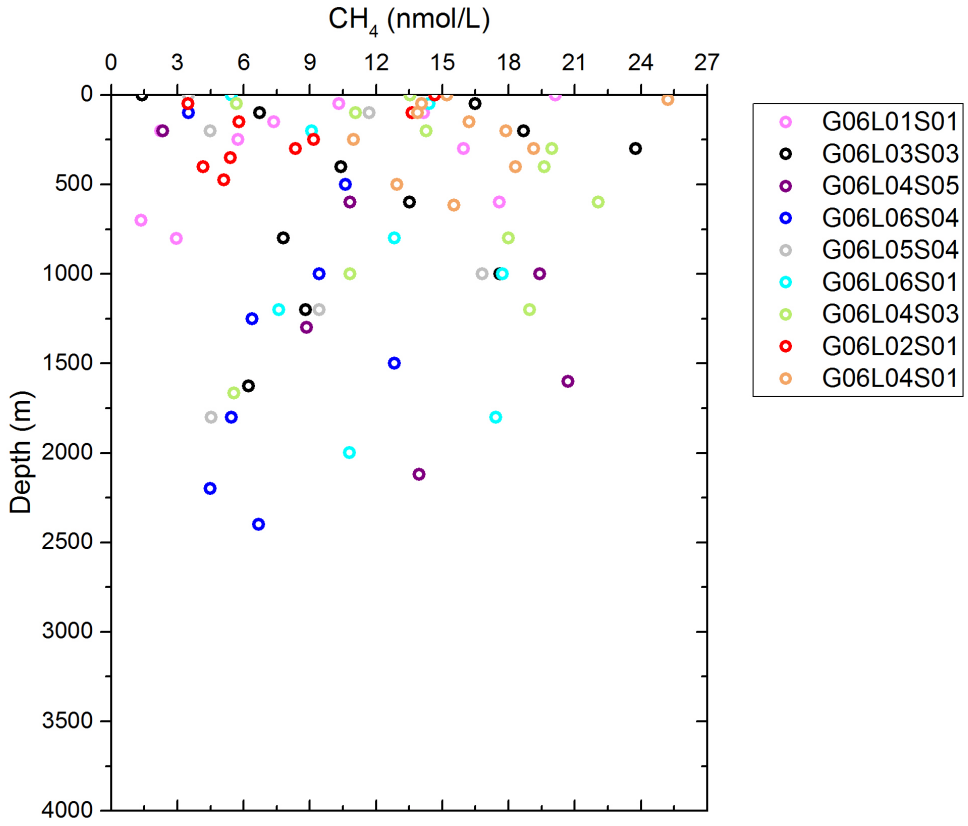

Figure 5: Methane concentrations from G06, represented by the circular symbols. The colors of the station symbols match those used in Figure 1 & 2 that showed station locations.

Dissolved Oxygen

Dissolved oxygen levels were measured by oxygen sensors on the CTD cast at every station, G05 levels are shown by Figure 6. The dissolved oxygen level never reached hypoxic levels, less than 1.4 mL/L [https://www.nwfsc.noaa.gov/research/divisions/fe/estuarine/oeip/de-hypoxia.cfm]. Methane concentrations were elevated in regions with lower dissolved oxygen minimums. Figure 7 displays the methane concentrations and dissolved oxygen levels for four stations that have the highest and lowest methane concentrations in G05.

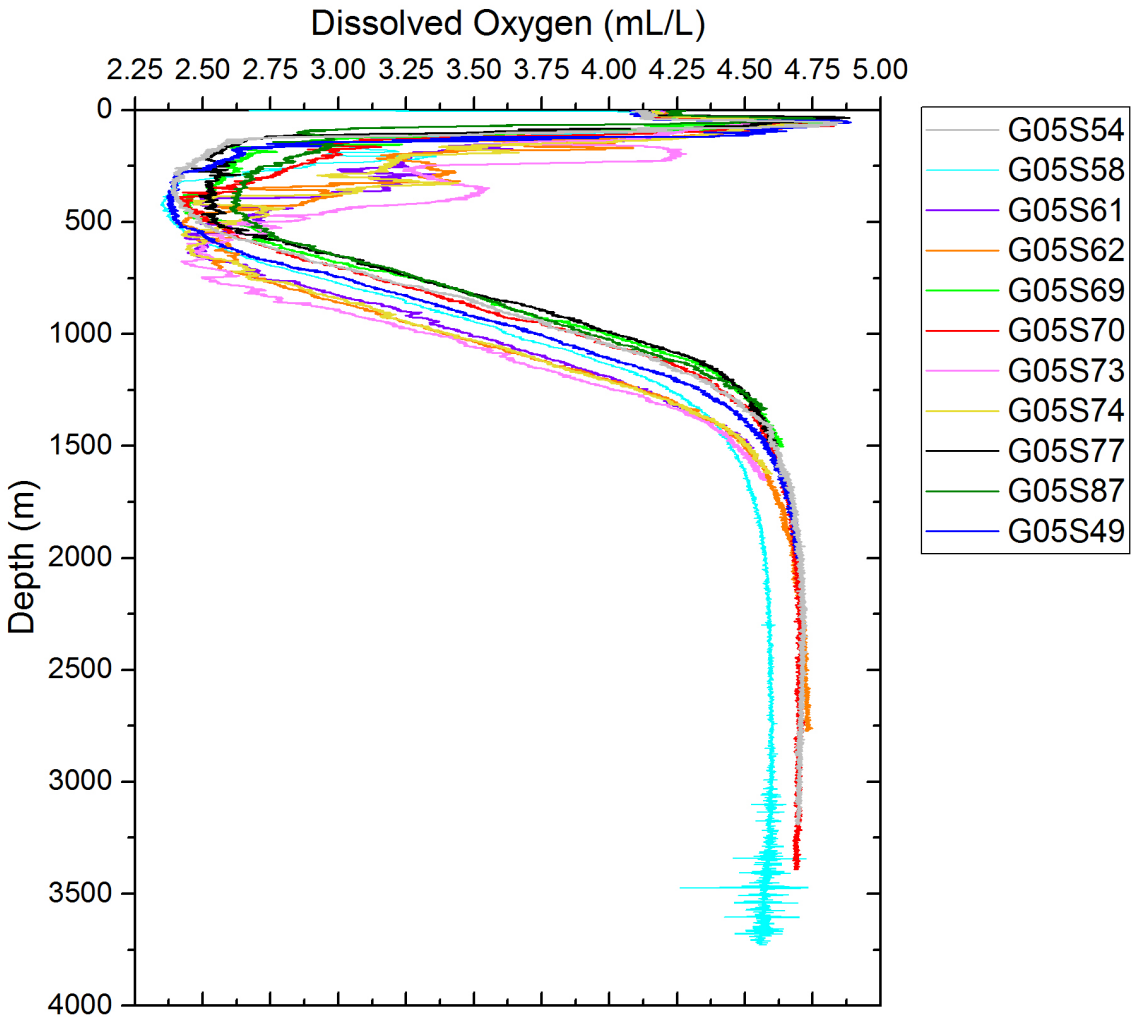

Figure 6: Dissolved Oxygen levels from all stations in G05. The line colors correspond with those of the station locations in Figure 1 & 2.

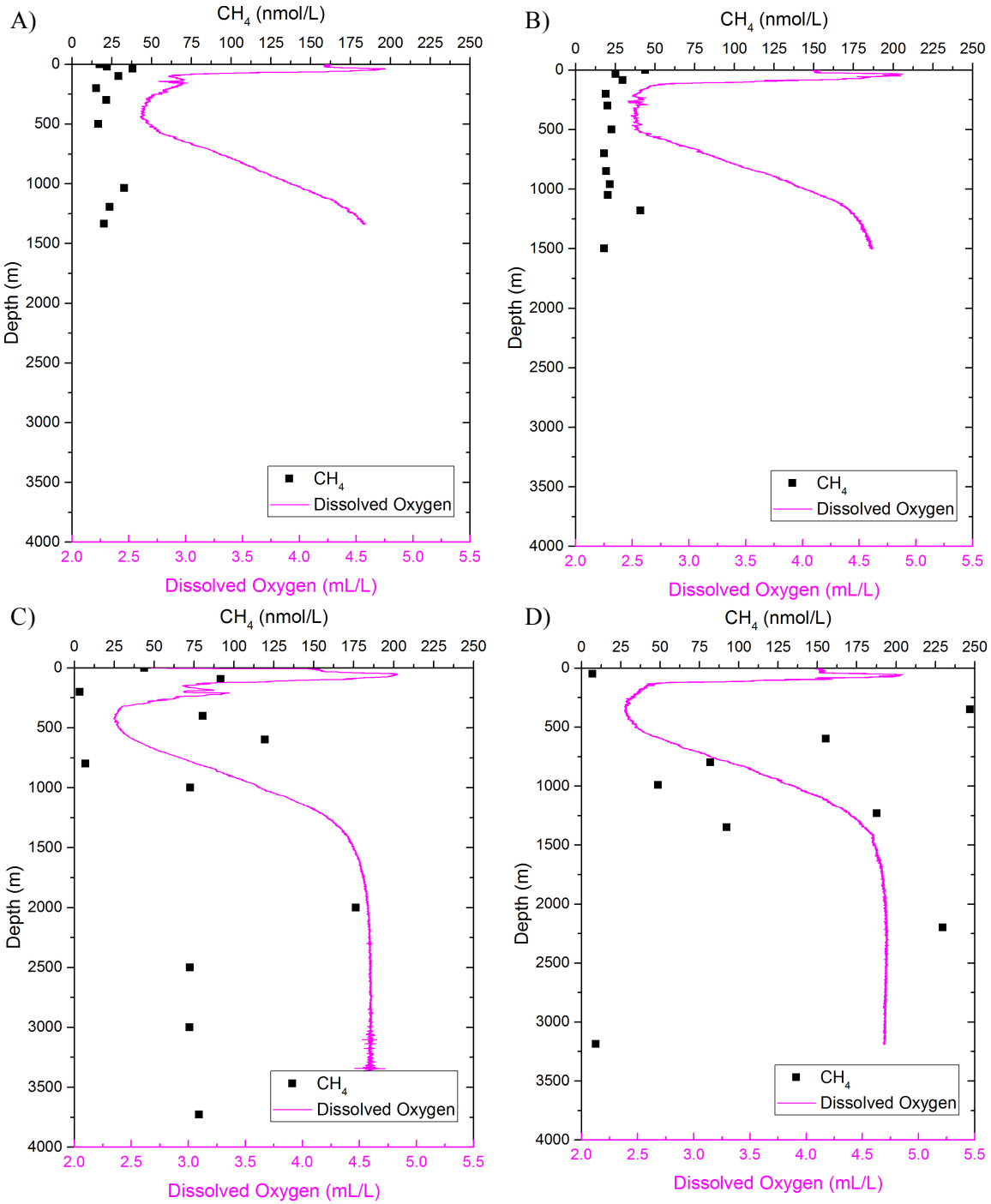

Figure 7: Dissolved oxygen levels and associated methane concentrations from the following stations A) G05S87 B) G05S77 C) G05S58 and D) G05S54.

Mixed Layer Depth

Northern Gulf of Mexico density depth profiles display the shallow mixed layer depth of around 19 meters (Figure 8). The western Gulf of Mexico had an average mixed layer depth of approximately 40 meters (Figure 8). This dictates what is considered maximum depth for usable surface concentrations for flux calculations.

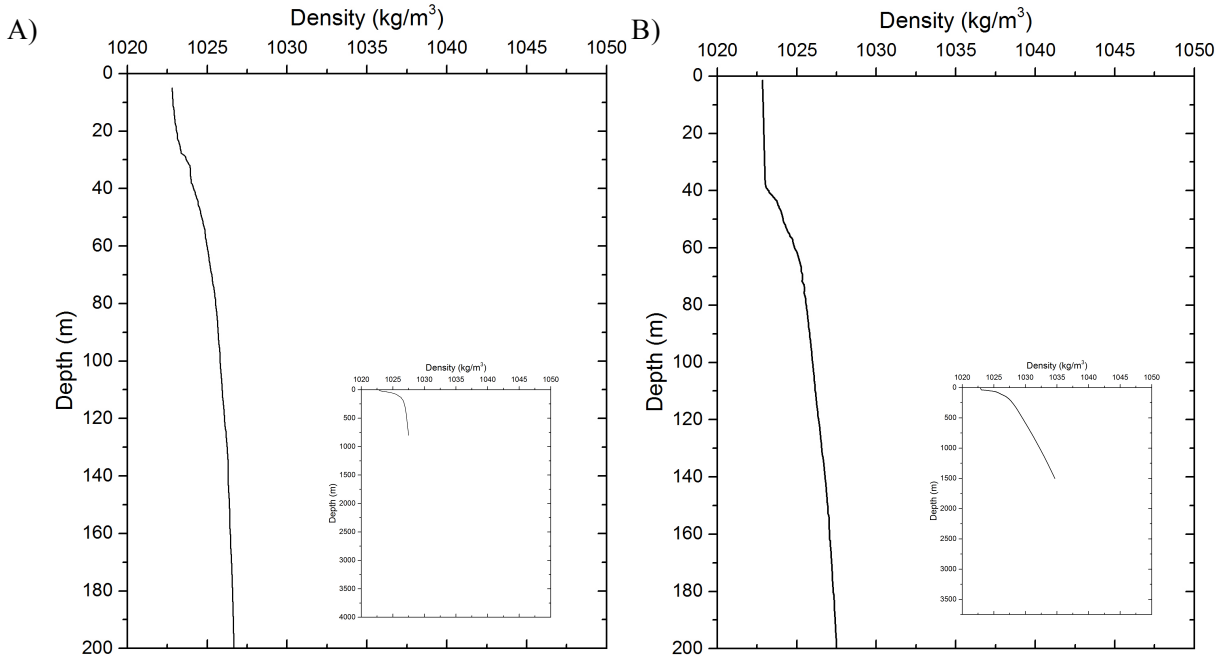

Figure 8: Representative density profiles from stations A) G06L01S01 (Northern Gulf of Mexico) and B) G05S69 (Western Gulf of Mexico).

Sea-to-Air Flux

Air-sea flux calculations were done for 17 of the 20 stations (Figure 9). Three stations did not have usable data within the mixed layer depth due to GC/FID errors, therefore no flux calculations could be done for those stations. Surface concentrations ranged from 1.4 to 84.9 nmol L^{-1}, with an average of 69.9 nmol L^{-1}. Calculated sea-to-air fluxes in the northern Gulf of Mexico ranged from -1.0 to 35.3 µmol m^{-2} d^{-1} with an average of 19.1 µmol m^{-2} d^{-1}. The western

Gulf of Mexico ranged from 36.4 to 202.2 µmol m^{-2} d^{-1} with an average of 115.2 µmol m^{-2} d^{-1}. The average flux including all calculated stations is 69.9 µmol m^{-2} d^{-1}. The maximum sea-to-air flux and surface concentration are from station G05S74. The minimums are from station G06L03S03, and this is the only station that is undersaturated with respect to the atmosphere.

There were two prior studies preformed in the northern Gulf of Mexico that reported on air-sea fluxes of CH_4, *Hu et al.* (2012) and *Solomon et al.* (2009). There was a three orders of magnitude difference in the numbers reported by each study (Table 5). The current study has calculated sea-to-air fluxes with the same magnitude as *Hu et al.* (2012) (Table 5). This study and *Solomon et al.* (2009) both used reported average atmospheric methane concentrations, while *Hu et al.* (2012) measured atmospheric mixing ratios during their cruise. *Hu et al.* (2012) collected their seawater surface samples within 4 meters of the surface, this study collected samples within 5 meters of the surface, and *Solomon et al.* (2009) sampled at depths of 20 meters or greater. *Solomon et al.* (2009) justified their sampling depth used for surface concentrations by stating the averaged mixed layer in summer is ~30 meters and ~80 meters in winter [*Solomon et al.,* 2009].

Table 5: Comparative Sea-to-Air Methane Fluxes

Study:	**Reported Fluxes (µmol d^{-1} m^{-2})**
This Study (Western Gulf of Mexico values)	36.4 to 202.2
This Study (Northern Gulf of Mexico values)	-1.0 to 35.3
Hu et al., 2012	-4.19 to 86.1
Solomon et al., 2009	200 to 10,500

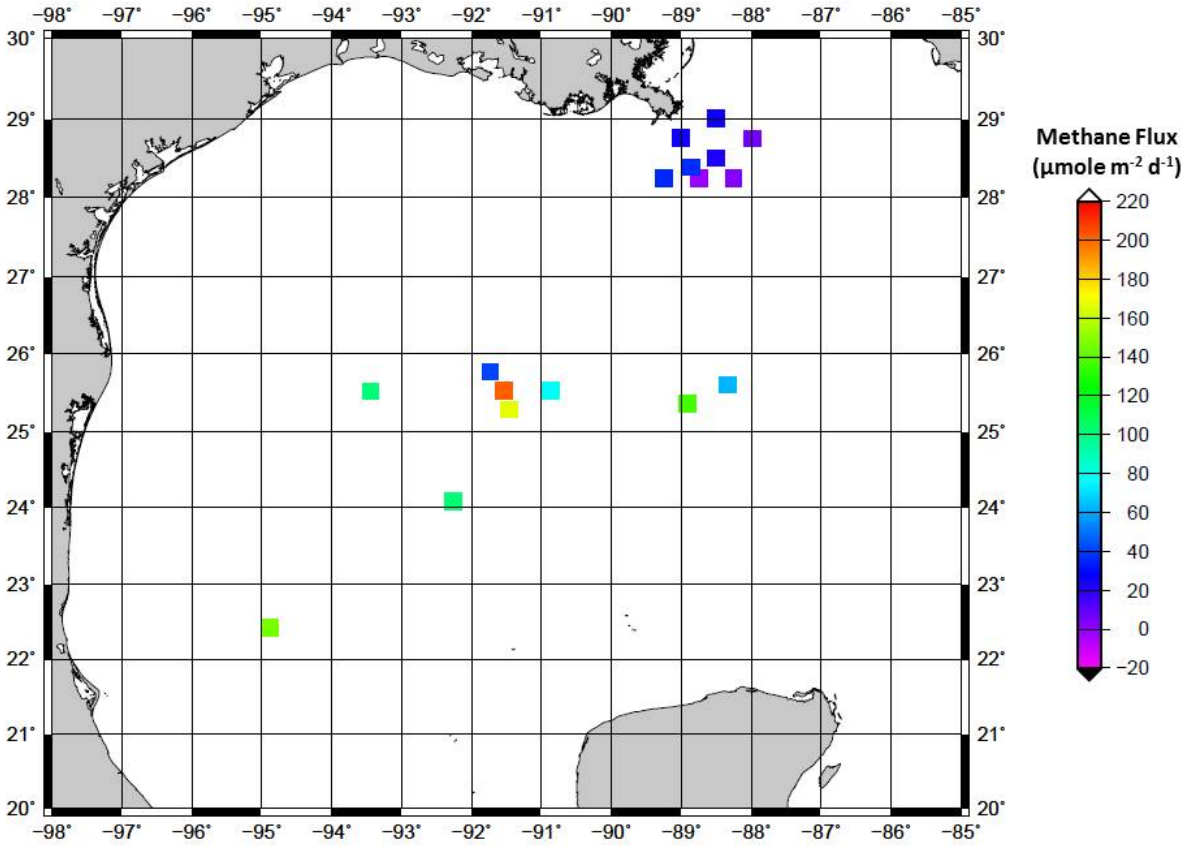

Figure 9: Air-sea flux of methane from 17 stations.

CHAPTER IV

CONCLUSION

The lack of measurable concentrations in the samples of ethane (C_2H_6) and propane (C_3H_8) suggests that there were no thermogenic methane sources for the methane observed in this study. Methane concentrations were elevated in regions with lower concentrations of dissolved oxygen at the oxygen minimum. The northern Gulf of Mexico mixed layer depth averaged 19 m and the Western Gulf of Mexico mixed layer depth averaged 40 m. Three stations did not have CH_4 concentrations within the mixed layer depth so no air-sea flux was determined for those stations. The calculated sea-to-air flux of CH_4 averaged 19.1 μmol m^{-2} d^{-1} in the Northern Gulf of Mexico and is in agreement with the findings of *Hu et al.* 2012. For the Western Gulf of Mexico, where there are no prior reported surface CH_4 data, the sea-to-air flux averaged 115.2 μmol m^{-2} d^{-1}. The overall average sea-to-air flux of methane is 69.9 μmol m^{-2} d^{-1}.

REFERENCES

Brown, I. J., R. Torres, A. P. Rees, (2014). The origin of sub-surface source waters define the sea–air flux of methane in the Mauritanian Upwelling, NW Africa. *Dynamics of atmospheres and oceans*, 67, 39-46.

Frank, D. J., W. Sackett, R. Hall (1970), Methane, Ethane, and Propane Concentrations in Gulf of Mexico. *AAPG bulletin*, 54(10), 1933-&.

Hu, L., S. A. Yvon Lewis, J. D. Kessler, I. R. MacDonald (2012). Methane fluxes to the atmosphere from deepwater hydrocarbon seeps in the northern Gulf of Mexico. *Journal of geophysical research*, 117(C1)

Karl, D. M., L. Beversdorf, K.M. Bjoerkman, M.J. Church, A. Martinez, K.M. Björkman, E.F. Delong (2008). Aerobic production of methane in the sea. *Nature Geoscience*, 1(7), 473-478.

Libes, S. M. (2009). Introduction to Marine Biogeochemistry. 2nd ed. Amsterdam: AP.

MacDonald, I. R., W. Sager, M. B. Peccini (2003). Gas hydrate and chemosynthetic biota in mounded bathymetry at mid-slope hydrocarbon seeps: Northern Gulf of Mexico. *Marine geology,* 198(1-2),133-158.

MacDonald, I. R., O. Garcia-Pineda, A. Beet, S. D. Asl, L. Feng, G. Graettinger, D. French-McCay, J. Holmes, C. Hu, F. Huffer, I. Leifer, F. Muller-Karger, A. Solow, M. Silva, G. Swayze (2015). Natural and unnatural oil slicks in the Gulf of Mexico. *Journal of Geophysical Research*, Oceans, 120(12), 8364-8380.

Mendes, S. D., M. C. Redmond, K. Voigritter, C. Perez, R. Scarlett, D. L. Valentine, (2015). Marine microbes rapidly adapt to consume ethane, propane, and butane within the dissolved hydrocarbon plume of a natural seep. *Journal of Geophysical Research*, Oceans, 120(3), 1937-1953.

Reeburgh, W. S. (2007). Oceanic Methane Biogeochemistry. *Chemical reviews*, 107(2), 486-513.

Solomon, E. A., M. Kastner, I. R. MacDonald, I. Leifer, (2009). Considerable methane fluxes to the atmosphere from hydrocarbon seeps in the Gulf of Mexico. *Nature Geoscience*, 2(8), 561-565.

Sweeney, C., E. Gloor, A. R. Jacobson, R. M. Key, G. McKinley, J. L. Sarmiento, R. Wanninkhof (2007). Constraining global air-sea gas exchange for CO_2 with recent bomb ^{14}C measurements. *Global Biogeochemical Cycles*, 21(2).

Tsunogai, U., A. Kosaka, N. Nakayama, D. D. Komatsu, U. Konno (2010). Origin and fate of deep-sea seeping methane bubbles at Kuroshima Knoll, Ryukyu forearc region, Japan. *Geochemical journal,* 44(6),461-476.

Wanninkhof, R. (1992). Relationship between wind speed and gas exchange over the ocean. *Journal of geophysical research*, 97(C5), 7373-7382.

Wiesenburg, D. A., L. N. Guinasso (1979). Equilibrium solubilities of methane, carbon monoxide, and hydrogen in water and sea water. *Journal of chemical & engineering data*, 24(4), 356-360.

Florida State University. http://www.met.fsu.edu/orgs/explores/atmcomp.html. May 15, 2015.

NOAA Earth System Research Laboratory, Global Monitoring Division. ftp://aftp.cmdl.noaa.gov/products/trends/ch4/ch4_mm_gl.txt. April 4, 2016.

NOAA Fisheries. https://www.nwfsc.noaa.gov/research/divisions/fe/estuarine/oeip/de-hypoxia.cfm. April 6, 2016.